Supporting Information for

Variations of atmospheric PAHs concentrations, sources, health risk, and direct medical costs of lung cancer around the Bohai Sea under the background of pollution prevention and control in China

Wenwen Ma[1,4,5], Rong Sun[1,4,*], Xiaoping Wang[3], Zheng Zong[1,4], Shizhen Zhao[2], Zeyu Sun[1,4,5], Chongguo Tian[1,4,*], Jianhui Tang[1,4], Song Cui[6], Jun Li[2], Gan Zhang[2]

[1] CAS Key Laboratory of Coastal Environmental Processes and Ecological Remediation, Yantai Institute of Coastal Zone Research, Chinese Academy of Sciences, Yantai Shandong 264003, P.R. China

[2] State Key Laboratory of Organic Geochemistry, Guangzhou Institute of Geochemistry, Chinese Academy of Sciences, Guangzhou, 510640, China

[3] Ludong University, Yantai, 264025, China

[4] Shandong Key Laboratory of Coastal Environmental Processes, Yantai Shandong 264003, P.R. China

[5] University of Chinese Academy of Sciences, Beijing, 100049, China

[6] International Joint Research Center for Persistent Toxic Substances (IJRC-PTS), School of Water Conservancy and Civil Engineering, Northeast Agricultural University, Harbin 150030, China

Correspondence to: Rong Sun (rsun@yic.ac.cn) and Chongguo Tian (cgtian@yic.ac.cn)

Content

Texts

Text S1. Calculation method of uncertainty input file

The uncertainty of the variables was calculated based on the method detection limit (MDL) and the concentration of each sample:

(1) for samples of which concentration lower than MDL, 5/6 of MDL was used as the corresponding uncertainty (Kim et al., 2004);

(2) for samples of which concentration higher than MDL, the uncertainty was calculated as following (Chueinta et al., 2000):

$$\sigma_{ij} = \frac{\mathrm{MDL}}{3} + cx_{ij} \quad (1)$$

where σ_{ij} is the uncertainty, MDL is the Method Detection Limit, x_{ij} is the concentration of the *i*th variable in the *j*th sample. *c* is the constant (0.1 when x_{ij} > 3MDL, 0.2 when x_{ij} < 3MDL).

Text S2. Positive Matrix Factorization (PMF)

PMF analyses involve many details about the development of the data, decisions of what data to include/exclude, determination of a solution, and evaluation of robustness of that solution; reporting of PMF solutions and analyses vary widely. The profiles obtained from the modeling must have physically meaningful results, i.e., there must be evidence of the potential sources in the study area. The analysis of the Q value (indicates the agreement of the model fit;) and the r^2 value (indicates the correlation between measured and estimated concentrations) can help to determine the best number of factors to be chosen for modeling (Wang et al., 2009). In this study, during the PMF analysis, the model was run for 3-7 factors and was always with random seeds. Finally, the five-factor solution was found to be ideal from 200 random bootstrapping and gave the most stable results and the most easily physically interpretable factors. The Q value (both robust and true) produced by this solution is close to the theoretical Q value, indicating that the PAHs data set in the modeling input provides appropriate uncertainty. The diagnostic regression R^2 value for the overall concentration of 228 samples is 0.9458, which is almost the same as the ratio of the predicted concentration of PMF to the measured concentration (Figure S6). It shows that the model results are good and

can be used as the basis for identifying the source of the target species. The r^2 values also show a good correlation, and the values of the scaled residuals were in the recommended range (-1.5 to +1.5). These parameters indicate that the modeling has provided good fitting results and that there was no significant outlier.

Text S3. Source identification

Factor 1 accounted for 9.4% of the Σ_{15} PAHs, the main load was HMW-PAHs such as BaP (85.0%), InD (84.5%), BghiP (46.8%), which was similar to the composition profile of vehicle emissions (He et al., 2008). BghiP and InD are regarded as markers of gasoline engines (Wu et al., 2014). In addition, the Fla/(Fla+Pyr) and InD/(InD+Bghip) of factor 1 were 0.30 and 0.50, respectively, the value less than 0.5 indicates that the main contribution came from vehicle exhaust (Characteristic PAH molecular diagnostic ratios were shown in Table S13 of SI). Therefore, factors 1 was interpreted gasoline vehicle emissions.

Factor 2 contributed 10.8% of the Σ_{15} PAHs, it was principally enriched the LMW-PAHs, Acy (57.6%) and Ace (77.4%). The composition of this factor was similar to the emission profiles of thermal power plant, steel plants and coking plants reported in the literature (Kong et al., 2013). Actually, there were industrial activities occurring in surrounding areas of the sites, such as sites in Tianjin, Liaoning, and Hebei Province. The inter-regional propagation of air masses has a great impact on the local concentration and distribution of PAHs in the air (Ma et al., 2010; Zhu et al., 2014) because of atmospheric diffusion and transport. Therefore, this factor was regarded as industrial processes.

Factor 3 accounted for the highest contribution of 49.6% of the Σ_{15} PAHs, it exhibited high loadings of Phe (93.8%), Ant (98.2%), Flu (62.5%) and moderate loadings of BaA (48.0%), Fla (26.2%), which corresponded to the profiles of incomplete combustion of coal (Huang et al., 2014; Chen et al., 2016). The ratios of Fla/(Fla+Pyr) and InD/(InD+Bghip) were 0.64 and 0.56, respectively, both greater than 0.5, and showed the characteristics of coal combustion emissions. Therefore, factor 3 was inferred to the coal combustion.

Factor 4 contributed 22.0%. Fla (59.3%) and Pyr (86.9%) are the dominant species, and moderate loadings of Chr (43.5%), which was similarly to the biomass emission components, such as straw, grass, wood (Shen et al., 2013; Ray et al., 2017). Maize and wheat are the two main crops in this area, and Fla and Pyr were the representative species of PAHs produced by straw burning (Jenkins et al., 1996). Therefore, factor 4 was identified as biomass burning.

Similarly to factor 1, factor 5 (8.2%) was mainly characterized by HMW-PAHs, which are recommended to be substantially emitted by diesel engines (Guarieiro et al., 2014). Factor 5 exhibited high loadings of BbF (80.2%), BkF (71.8%), DahA (57.4%), BaA (47.2%). BbF and BkF were regarded as characteristic compounds of diesel emissions (Zhu et al., 2003; Riddle et al., 2007; He et al., 2008), the diesel vehicle or ship exhaust was considered to have high loading of BkF. And the Fla/(Fla+Pyr) and InD /(InD+Bghip) of factor 5 were 0.48 and 0.20, respectively, that was suggested to the diesel exhaust (Gong et al., 2018). Therefore, factor 5 was respectively classified as diesel vehicle exhaust.

Tables

Table S1. Sampling information for 12 sampling sites (geographical location and sampling days)

Year	Sampling Sites	Beihuang	Dalian	Donggang	Dongying	Gaizhou	Longkou	Laoting	Rongcheng	Tianjin	Xingcheng	Yantai	Zhuanghe
	Abbr.	BH	DL	DG	DY	GZ	LK	LT	RC	TJ	XC	YT	ZH
	Longitude (E)	120.92	121.53	123.89	118.92	122.16	120.27	119.06	122.69	117.44	120.58	121.43	122.99
	Latitude (N)	38.4	38.87	39.85	37.5	40.25	37.69	39.34	37.39	38.84	40.47	37.59	39.64
2014	Summer	-	76	80	69	92	-	79	87	75	77	71	77
2014	Autumn	91	89	90	92	74	93	91	94	115	90	93	67
2014	Winter	-	98	84	92	88	91	92	89	89	94	91	88
2015	Spring	-	92	108	106	103	109	105	108	106	99	106	100
2015	Summer	104	81	81	82	81	82	81	82	81	82	82	81
2015	Autumn	76	97	97	97	102	97	97	97	98	97	101	97
2015	Winter	-	92	94	86	91	85	92	90	87	90	86	93
2016	Spring	90	90	87	84	83	84	84	84	86	87	-	88
2016	Summer	88	85	85	87	87	87	83	91	83	86	86	90
2016	Autumn	90	101	-	99	99	100	101	106	100	103	99	96
2016	Winter	85	97	99	91	96	90	93	95	93	93	91	97
2017	Spring	102	82	81	94	82	97	89	-	92	87	87	82
2017	Summer	68	93	89	87	88	85	87	91	85	84	94	93
2017	Autumn	120	89	94	95	94	97	95	105	97	98	98	89
2017	Winter	84	97	97	92	93	92	93	89	95	95	88	97
2018	Spring	92	79	79	82	79	82	81	83	78	79	83	79
2018	Summer	-	101	100	93	103	94	100	93	96	98	91	100
2018	Autumn	92	96	98	101	94	99	89	101	102	95	101	98
2018	Winter	-	84	83	80	-	81	91	81	81	88	81	83
2019	Spring	-	89	88	91	88	92	88	91	88	88	92	88
Numbers of sampler		13	20	19	20	19	19	20	19	20	20	19	20

-:Missing sample.

Table S2. The ring numbers, method detection limits (MDLs), TEF_i, and other information for PAHs in this study

The target compounds (abbreviation)	Ring Numbers	MDLs (ng sample^{-1})	TEF_i [a]	Standard curve	Correlations
Acenaphthylene(Acy)	3	0.126	0.001	y=6326.2x+16600	0.9930
Acenapthene (Ace)	3	0.103	0.001	y=4837.4x+31320	0.9999
Fluorene (Flu)	3	0.089	0.001	y=24634x+44631	0.9998
Phenanthrene (Phe)	3	0.078	0.001	y=97525x+43017	0.9913
Anthracene (Ant)	3	0.044	0.01	y=96301x+5130.4	0.9958
Fluoranthene (Fla)	4	0.017	0.001	y=210183x-79803	0.9977
Pyrene (Pyr)	4	0.026	0.001	y=209836x-75917	0.9979
Benzo[a]anthracene (BaA)	4	0.025	0.1	y=238735x-141456	0.9948
Chrysene (Chr)	4	0.041	0.01	y=159007x-74207	0.9928
Benzo[b]fluoranthene (BbF)	5	0.062	0.1	y=283344x-180199	0.9982
Benzo[k]fluoranthene (BkF)	5	0.055	0.1	y=254895x-111330	0.9961
Benzo[a]pyrene (BaP)	5	0.016	1	y=233835x-119274	0.9986
Dibenzo[a,h]anthracene (DahA)	5	0.048	1	y=126081x-124963	0.9962
Indeno[1,2,3-cd]pyrene (InD)	6	0.032	0.1	y=240503x-180428	0.9961
Benzo[ghi] perylene (BghiP)	6	0.070	0.01	y=253793x-174580	0.9990

[a]: The toxic equivalency factors (TEFs) (Nisbet and Lagoy, 1992).x is the concentration of PAH, loaded on the gas sample which detected; y is the peak area of target compound.

Table S3. The annual concentration of PAHs around Bohai Sea (Mean±SD, ng m^{-3})

Compound	Summer 2014 to Spring 2015	Summer 2015 to Spring 2016	Summer 2016 to Spring 2017	Summer 2017 to Spring 2018	Summer 2018 to Spring 2019	Five-year
Acy	0.63±0.26	0.86±0.56	0.73±0.37	1.07±0.72	1.14±0.86	0.89±0.22
Ace	0.54±0.07	0.84±0.28	1.33±0.66	1.45±1.06	1.52±0.87	1.13±0.42
Flu	4.18±3.00	6.51±6.30	6.60±3.98	8.63±7.50	9.40±6.88	6.97±1.92
Phe	25.6±18.1	26.2±16.1	24.2±17.5	18.1±6.64	14.9±9.2	21.6±5.8
Ant	2.44±1.95	2.48±2.12	2.19±1.29	2.91±2.08	3.43±2.11	2.67±0.46
Fla	11.8±5.60	8.08±4.88	13.3±4.89	10.9±6.63	12.4±6.6	11.24±2.05
Pyr	7.60±3.47	1.47±0.73	8.49±2.97	6.37±3.82	7.47±3.83	6.26±2.8
BaA	1.16±0.55	1.29±0.30	0.75±0.38	0.66±0.55	0.78±0.60	0.92±0.29
Chr	1.65±0.44	1.37±0.27	1.39±0.49	1.12±0.64	1.20±0.62	1.35±0.22
BbF	1.83±0.44	1.46±0.20	0.46±0.27	0.26±0.26	0.47±0.33	0.89±0.71
BkF	1.15±0.20	0.78±0.09	0.29±0.11	0.29±0.25	0.55±0.35	0.61±0.36
BaP	0.86±0.17	1.14±0.43	0.34±0.28	0.32±0.16	0.18±0.18	0.57±0.42
DahA	1.03±0.42	0.74±0.42	0.07±0.04	0.06±0.05	0.04±0.02	0.39±0.47
InD	1.22±0.57	1.74±0.75	0.32±0.18	0.24±0.26	0.21±0.14	0.74±0.69
BghiP	1.07±0.67	1.10±0.20	0.27±0.17	0.20±0.20	0.26±0.18	0.58±0.46
$\sum_{15}$ PAHs	63.6±58.4	55.5±37.9	60.9±31.1	51.4±29.4	52.5±40.1	56.8±4.80
LMW-PAHs	34.0±18.8	36.4±29.8	35.1±22.4	31.6±24.1	29.0±28.5	33.2±6.81
MMW-PAHs	22.5±18.5	12.1±9.82	24.0±19.9	18.6±11.6	21.6±11.4	19.8±4.70
HMW-PAHs	7.18±3.32	6.93±3.28	1.76±1.80	1.19±2.12	1.81±2.15	3.78±2.69

Table S4. Significance level between annual mean concentration of PAHs by t-test

	year 1-year 2	year 2-year 3	year 3-year 4	year 4-year 5
Σ_{15} PAHs	0.541	0.477	0.139	0.142
3-ring	0.809	0.768	0.168	0.067
4-ring	**0.002**	**0.001**	0.152	0.575
5-ring	0.055	**0.000**	0.108	0.056
6-ring	0.133	**0.000**	0.219	0.813

Note: Bold: $p<0.05$, the difference is significant.

Table S5. The seasonal concentration of PAHs (Mean±SD, ng m^{-3})

Compound	Spring	Summer	Autumn	Winter
Acy	0.48±0.19	0.42±0.2	1.75±0.56	0.89±0.4
Ace	0.72±0.25	0.88±0.84	1.31±0.60	1.63±1.15
Flu	2.95±1.71	1.95±1.06	7.60±2.23	15.8±5.19
Phe	18.8±12.01	9.26±4.61	17.2±5.83	41.4±14.3
Ant	1.28±0.76	0.65±0.14	3.41±0.64	5.43±0.95
Fla	9.08±5.54	5.84±4.52	11.0±1.57	19.2±2.68
Pyr	4.94±3.37	3.77±3.75	6.14±2.64	10.3±4.38
BaA	0.61±0.34	0.50±0.37	0.91±0.31	1.69±0.24
Chr	1.27±0.38	0.84±0.42	1.23±0.31	2.05±0.27
BbF	0.81±0.74	0.61±0.63	0.80±0.75	1.37±0.74
BkF	0.64±0.44	0.42±0.38	0.51±0.39	0.88±0.37
BaP	0.42±0.30	0.31±0.33	0.63±0.58	0.91±0.48
DahA	0.40±0.53	0.13±0.16	0.38±0.47	0.64±0.73
InD	0.74±0.83	0.38±0.35	0.62±0.79	1.24±1.00
BghiP	0.72±0.82	0.32±0.34	0.40±0.42	0.88±0.47
$\sum_{15}$ PAHs	43.9±19.5	26.3±13.4	53.9±9.10	104.3±9.50
LMW-PAHs	24.3±14.7	13.2±6.62	31.3±8.03	65.2±12.1
MMW-PAHs	15.9±8.93	11.0±8.48	19.3±3.93	33.3±7.10
HMW-PAHs	3.73±3.53	2.17±2.14	3.34±3.10	5.93±3.51

Table S6. Significant difference between seasonal PAHs concentration and ring number by t-test

Compound	Spring-Summer	Summer-Autumn	Autumn-Winter	Winter-Spring
Σ_{15}PAHs	**0.000**	**0.000**	**0.000**	**0.000**
3-ring	**0.000**	**0.000**	**0.000**	**0.000**
4-ring	**0.035**	**0.003**	**0.000**	**0.000**
5-ring	**0.005**	**0.007**	**0.001**	**0.001**
6-ring	**0.001**	0.123	**0.000**	**0.045**

Table S7. The annual average daily concentration of 15 PAHs at 12 sampling sites from June 2014 to May 2019 (Mean±SD, ng m^{-3})

Compounds	BH	DL	DG	DY	GZ	LK	LT	RC	TJ	XC	YT	ZH
Acy	0.61±0.20	0.61±0.20	0.83±0.37	0.47±0.08	1.39±0.52	0.35±0.24	1.28±0.47	0.46±0.07	0.76±0.20	2.22±0.78	0.46±0.08	1.18±0.58
Ace	0.82±0.24	0.82±0.24	1.45±0.79	0.65±0.18	1.60±0.65	0.69±0.45	1.34±0.52	0.86±0.25	1.42±0.66	1.64±0.59	0.75±0.24	1.28±0.57
Flu	3.95±0.61	3.95±0.61	8.10±3.57	4.05±0.80	9.80±2.32	4.81±1.22	10.1±3.15	3.25±1.03	5.85±1.20	15.5±5.59	3.73±1.44	9.31±4.42
Phe	14.3±2.36	14.3±2.36	27.05±8.31	11.4±2.28	45.2±15.9	14.8±4.18	40.6±10.4	9.96±4.05	23.3±6.57	32.7±27.4	13.8±3.85	37.9±12.8
Ant	1.07±0.30	1.07±030	2.83±1.44	0.73±0.23	5.72±1.99	1.05±0.35	3.69±0.95	0.90±0.34	1.24±0.22	8.30±3.84	0.91±0.28	3.98±1.76
Fla	5.30±1.43	5.30±1.43	12.5±3.55	5.65±1.17	22.3±6.69	7.11±2.72	16.8±4.13	4.67±1.70	11.1±4.47	20.9±4.31	7.23±1.78	13.6±4.56
Pyr	2.78±1.38	2.78±1.38	6.91±3.17	2.28±0.86	13.5±6.45	3.77±2.22	9.43±4.09	2.40±1.07	5.64±3.81	12.1±5.26	3.33±1.00	8.80±4.14
BaA	0.54±0.40	0.54±0.40	0.97±0.32	0.52±0.34	1.59±0.48	0.46±0.10	1.15±0.27	0.47±0.31	0.79±0.46	2.09±0.60	0.58±0.37	1.19±0.27
Chr	0.84±0.44	0.84±0.44	1.25±0.47	0.99±0.22	2.30±0.60	0.95±0.38	1.68±0.23	0.83±0.25	1.43±0.72	2.21±0.44	1.05±0.29	1.45±0.32
BbF	0.70±0.69	0.70±0.69	0.86±0.54	0.73±0.63	1.25±0.63	0.68±0.48	0.98±0.67	0.65±0.60	0.86±0.72	1.33±0.79	0.74±0.65	1.07±0.79
BkF	0.46±0.42	0.46±0.42	0.65±0.29	0.50±0.36	0.83±0.24	0.44±0.25	0.69±0.33	0.43±0.35	0.57±0.38	0.99±0.50	0.52±0.35	0.70±0.47
BaP	0.32±0.27	0.32±0.27	0.45±0.21	0.34±0.26	0.90±0.53	0.44±0.37	0.88±0.60	0.21±0.30	0.72±0.62	0.91±0.49	0.59±0.57	0.61±0.40
DahA	0.17±0.19	0.17±0.19	0.34±0.35	0.25±0.28	0.54±0.54	0.54±0.69	0.56±0.64	0.17±0.15	0.57±0.69	0.62±0.64	0.36±0.49	0.28±0.34
InD	0.59±0.60	0.59±0.60	0.72±0.49	0.55±0.52	1.04±0.77	0.38±0.25	1.04±0.91	0.36±0.36	0.91±0.89	1.35±1.21	0.69±0.72	0.69±0.53
BghiP	0.42±0.42	0.42±0.42	0.48±0.29	0.58±0.56	0.76±0.43	0.52±0.41	0.66±0.43	0.31±0.27	0.66±0.58	0.89±0.51	0.57±0.54	0.54±0.37
$\sum_{15}$PAHs	27.5±10.9	32.9±7.03	65.4±9.68	29.7±3.68	98.8±27.8	37.0±9.60	90.8±17.1	25.9±6.41	55.8±16.9	103.7±39.1	35.3±7.58	72.5±25.4
LMW-PAHs	16.9±6.94	20.8±2.54	40.3±7.47	17.3±3.32	53.7±16.0	21.7±5.97	57.0±11.7	15.4±5.25	32.5±7.17	60.3±34.7	19.6±5.44	43.6±18.9
MMW-PAHs	8.81±5.10	9.46±3.14	21.6±6.91	9.44±1.83	39.7±13.9	12.3±5.24	29.0±7.90	8.37±2.66	18.9±8.83	37.3±9.57	12.2±2.28	25.0±8.89
HMW-PAHs	1.89±1.45	2.68±2.52	3.52±2.05	3.00±2.51	5.43±2.89	3.06±2.32	4.90±3.35	2.18±1.72	4.35±3.72	6.27±3.65	3.52±3.03	3.97±2.68

Table S8. Pearson correlation coefficients of the proportion of different ring number of PAHs among 12 sampling sites from June 2014 to May 2019

	BH	DL	DG	DY	GZ	LT	LK	RC	TJ	XC	YT	ZH
BH	1											
DL	.99**	1										
DG	.99**	.99**	1									
DY	.99**	.99**	.99**	1								
GZ	.98**	.98**	.99**	.98**	1							
LT	.98**	.99**	.99**	.99**	.99**	1						
LK	.99**	.99**	.99**	.99**	.99**	.99**	1					
RC	.99**	.99**	.99**	.99**	.99**	.99**	.99**	1				
TJ	.98**	.99**	.99**	.99**	.99**	.99**	.99**	.99**	1			
XC	.97**	.99**	.99**	.98**	.98**	.99**	.98**	.98**	.98**	1		
YT	.98**	.98**	.99**	.99**	.99**	.99**	.99**	.99**	.99**	.98**	1	
ZH	.97**	.99**	.99**	.98**	.99**	.99**	.99**	.99**	.99**	.99**	.98**	1

Note: **. at the 0.05 level (two-tailed), the correlation is significant, * at the 0.01 level (two-tailed), the correlation is significant.

Table S9. Pearson correlation coefficient of 20 seasonal concentrations of PAHs at Tianjin and the four adjacent sites

	TJ	LT	DY	LK	XC
TJ	1				
LT	0.50*	1			
DY	0.61*	0.89**	1		
LK	0.66**	0.73**	0.75**	1	
XC	0.68**	0.79**	0.72**	0.77**	1

Note: **. at the 0.01 level (two-tailed), the correlation is significant.

Table S10. VARIMAX-rotated factor loadings of PCA of atmospheric PAHs at the BS

PAHs	PC1	PC2	PC3	PC4
Ace	-0.057	**0.631**	0.003	**0.678**
Acy	0.050	0.154	0.266	**0.830**
Flu	0.157	0.510	0.553	0.498
Ant	0.228	0.394	**0.690**	0.470
Phe	0.255	0.325	**0.867**	0.123
BaA	0.548	0.560	0.462	0.303
Chr	0.517	**0.694**	0.324	0.214
Fla	0.217	**0.819**	0.400	0.241
Pyr	0.047	**0.930**	0.219	0.141
BaP	**0.826**	0.048	0.343	0.110
BkF	**0.827**	0.474	0.095	0.094
DahA	**0.859**	-0.009	0.033	-0.110
InD	**0.886**	-0.042	0.302	0.202
BbF	**0.909**	0.297	0.200	0.005
BghiP	**0.932**	0.168	-0.006	0.038
Explained variance (%)	35.657	24.130	15.925	12.828
Sum explained variance (%)	35.657	59.787	75.712	88.540

Note: The bold value indicates that the PCA load is greater than 0.6.

Table S11. Characteristic PAH molecular diagnostic ratios

	Petrogenic	Petroleum combustion	Grass, wood, coal combustion	Reference
Fla/(Fla+Pyr)	<0.4	0.4–0.5	>0.5	(Westerholm et al., 2001; Yunker et al., 2002; Tobiszewski and Namiesnik, 2012)
InD /(InD+Bghip)	<0.2	0.2-0.5	>0.5	

Table S12. The seasonal mean concentration of $PM_{2.5}$ (μg m^{-3}) and PAHs (ng m^{-3})

sites	DG		DL		DY		GZ		LT		TJ		XC		YT	
seasons	$PM_{2.5}$	PAHs	$PM_{2.5}$	PAHs	$PM_{2.5}$	PAHs	$PM_{2.5}$	PAHs	$PM_{2.5}$	PAHs	$PM_{2.5}$	PAHs	$PM_{2.5}$	PAHs	$PM_{2.5}$	PAHs
2014 summer	35	25	43	8	60	16	30	45	77	35	64	55	48	49	44	16
2014 autumn	44	56	49	29	73	26	37	172	96	82	89	74	45	123	42	31
2014 winter	61	117	54	70	87	70	53	288	102	178	96	103	65	191	55	74
2015 spring	47	43	44	20	73	17	47	78	90	53	62	42	55	52	47	21
2015 summer	29	18	31	12	59	10	28	31	63	31	53	33	45	25	32	19
2015 autumn	47	69	50	26	76	25	54	79	71	97	62	88	42	215	36	43
2015 winter	56	88	58	84	104	45	63	126	91	153	83	117	60	396	59	66
2016 spring	50	22	44	14	64	21	42	41	65	30	65	73	46	35	44	--
2016 summer	28	85	24	28	41	11	28	89	51	36	49	20	36	119	25	18
2016 autumn	38	--	36	24	65	30	49	167	82	65	73	46	46	91	36	34
2016 winter	54	114	54	49	96	76	74	212	121	175	110	108	78	281	54	42
2017 spring	42	13	38	32	54	19	38	59	60	69	58	41	43	53	37	18
2017 summer	20	19	24	11	38	11	28	27	44	31	45	20	37	34	25	15
2017 autumn	29	48	27	20	50	25	36	82	62	82	56	36	38	100	27	29
2017 winter	44	194	38	71	67	45	62	119	67	142	61	65	58	148	41	46
2018 spring	31	44	31	18	47	19	41	126	59	59	52	30	41	27	29	12
2018 summer	16	14	19	8	27	8	20	33	41	21	36	14	25	10	19	11
2018 autumn	26	36	28	11	45	28	39	172	58	115	51	35	40	280	24	22
2018 winter	50	141	45	42	73	56	61	--	73	186	71	62	62	325	57	71
2019 Spring	38	91	40	31	45	33	41	122	51	174	48	21	45	116	35	74

The data of $PM_{2.5}$ from https://www.aqistudy.cn/historydata/;--: Missing sample

Table S13. The Pearson correlation of concentration between $PM_{2.5}$ and PAHs

sites	DG	DL	DY	GZ	LT	TJ	XC	YT
Pearson correlation	.537*	.637**	.724**	.600**	.485*	.868**	.705**	.682**
Sig. (two- tailed)	0.018	0.003	0.000	0.007	0.030	0.000	0.001	0.001
Number of cases	19	20	20	19	20	20	20	19

**. At the 0.01 level (two-tailed), the correlation is significant.

Table S14. The annual mean of ILCR caused by PAHs exposure around the BS and TJ from June 2014 to May 2019

Area	2014-2015	2015-2016	2016-2017	2017-2018	2018-2019	Average
BS	2.22×10^{-4}	2.16×10^{-4}	5.86×10^{-4}	$4..07\times10^{-5}$	5.70×10^{-5}	1.19×10^{-4}
TJ	3.16×10^{-4}	2.94×10^{-4}	7.33×10^{-5}	2.39×10^{-5}	2.72×10^{-5}	1.47×10^{-4}

Table S15. Annual average TEQ of atmospheric PAHs around the BS from June 2014 to May 2019

Year	TEQ	BaP	DahA	TEQ-BaP%	TEQ-DahA%
2014–2015	2.55±1.49	0.87±0.56	1.04±0.87	31.5±23.6	29.5±24.0
2015–2016	2.49±1.63	1.14±0.84	0.73±0.73	36.0±27.7	20.8±22.2
2016–2017	0.69±0.76	0.34±0.44	0.07±0.07	42.7±16.1	11.8±7.1
2017–2018	0.46±0.66	0.17±0.27	0.06±0.1	37.5±11.2	12.7±8.0
2018–2019	0.67±0.84	0.32±0.43	0.04±0.06	43.3±15.6	8.3±11.6
Average	1.37±1.05	0.57±0.41	0.39±0.47	38.2±8.0	16.6±9.0

Note: TEQ-BaP% and TEQ-DahA% represent the proportion of BaP and DahA in TEQ, respectively.

Table S16. The direct medical costs of lung cancer caused by PAHs exposure around the BS

Year	rr	URR	PAF	I_{add}	Population (persons)	C_t (USD)
2014	1.0027	4.49	2.68‰	2.34×10^{-6}	2.29×10^{8}	4.35×10^{6}
2015	1.0026	4.49	2.61‰	2.28×10^{-6}	2.30×10^{8}	4.27×10^{6}
2016	1.0007	4.49	0.73‰	6.36×10^{-7}	2.32×10^{8}	1.20×10^{6}
2017	1.0005	4.49	0.49‰	4.25×10^{-7}	2.33×10^{8}	8.03×10^{5}
2018	1.0007	4.49	0.70‰	6.15×10^{-7}	2.34×10^{8}	1.17×10^{5}
Average	1.0014	4.49	1.44‰	1.26×10^{-6}	2.32×10^{8}	3.36×10^{6}

Note: The population data derives from: http://tjj.ln.gov.cn/tjsj/sjcx/ndsj/, http://tjj.hebei.gov.cn/hetj/tjsj/jjnj/, http://tjj.shandong.gov.cn/col/col104011/index.html?jh=263.

Table S17. The direct medical costs of lung cancer caused by PAHs exposure at TJ

Year	rr	URR	PAF	I_{add}	Population (persons)	C_t (USD)
Year 1	1.0038	4.49	3.81‰	3.33×10^{-6}	1.52×10^{7}	4.39×10^{5}
Year 2	1.0036	4.49	3.54‰	3.10×10^{-6}	1.55×10^{7}	4.17×10^{5}
Year 3	1.0009	4.49	0.89‰	7.73×10^{-7}	1.56×10^{7}	1.05×10^{5}
Year 4	1.0003	4.49	0.29‰	2.53×10^{-7}	1.56×10^{7}	3.42×10^{4}
Year 5	1.0003	4.49	0.33‰	2.87×10^{-7}	1.56×10^{7}	3.90×10^{4}
Average	1.0018	4.49	1.77‰	1.55×10^{-6}	1.55×10^{7}	2.07×10^{5}

Note: The population data derives from: http://stats.tj.gov.cn/tjsj_52032/tjnj/.

Figures

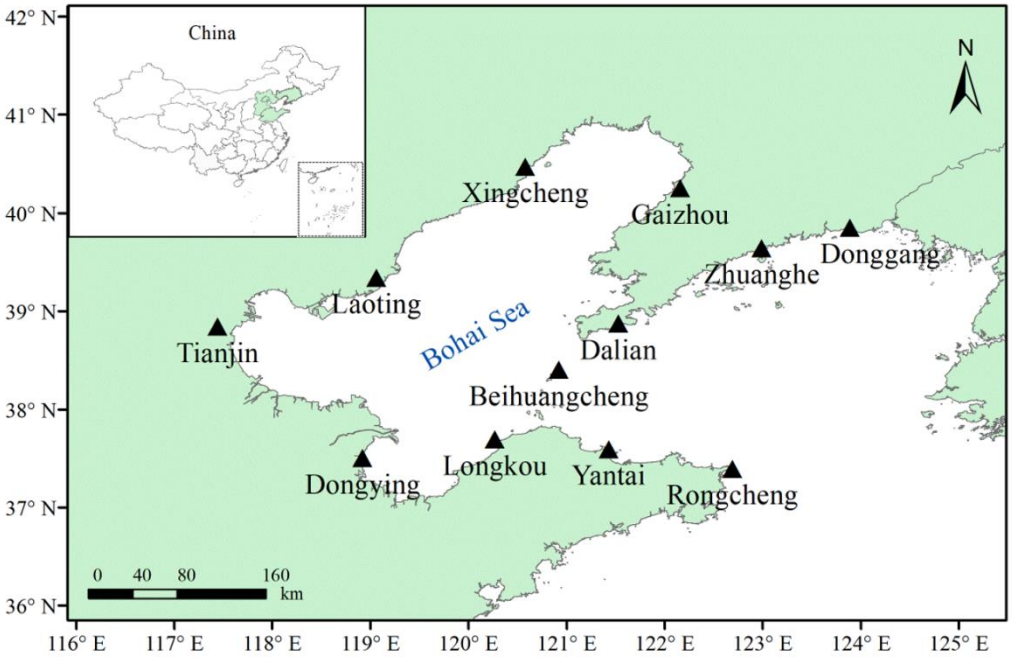

Figure S1. The locations of the 12 sampling sites around the BS.

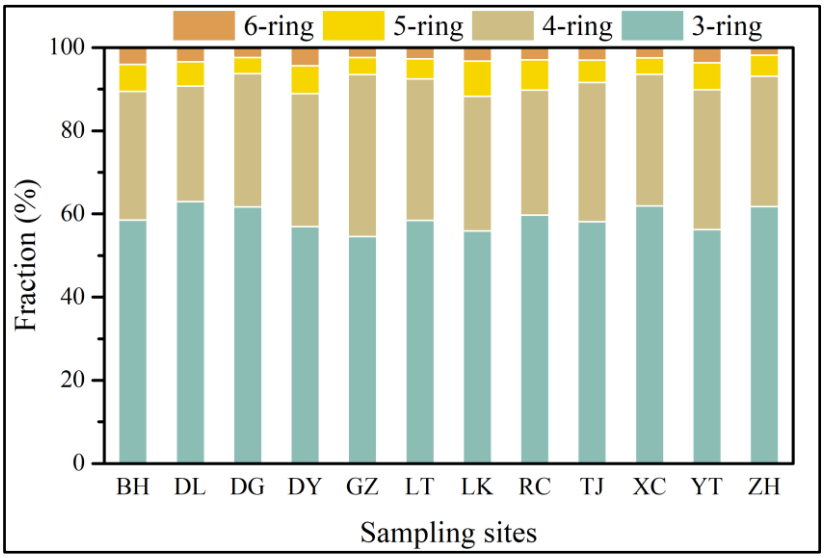

Figure S2. The five-year average fractions of different rings of $\sum_{15}$ PAHs at 12 sampling sites.

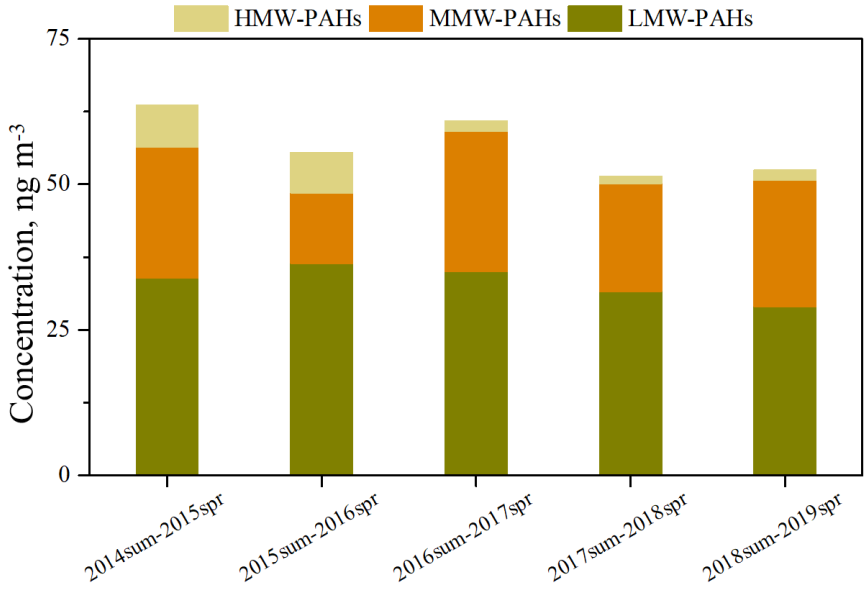

Figure S3. The annual average concentration of PAHs sub-rings around the BS.

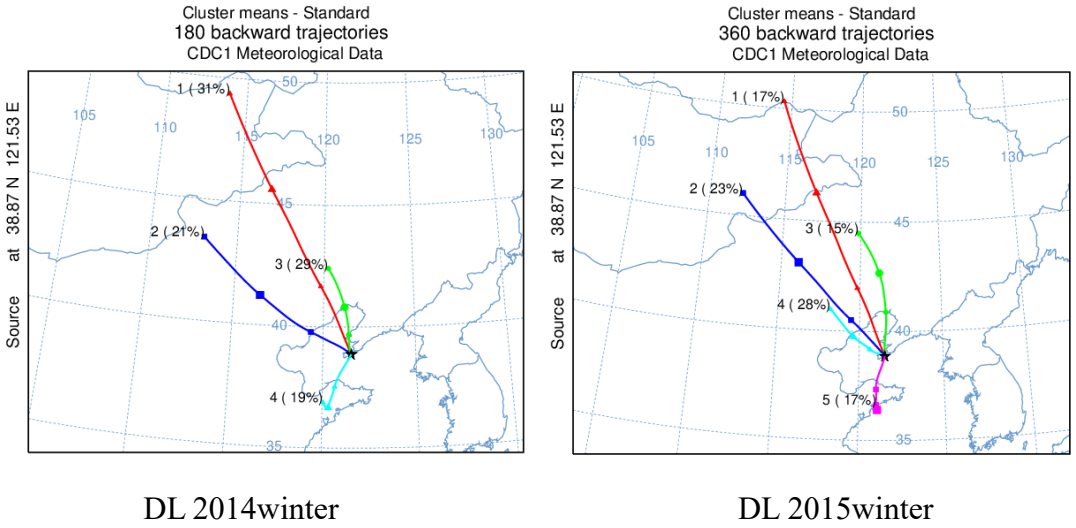

DL 2014winter DL 2015winter

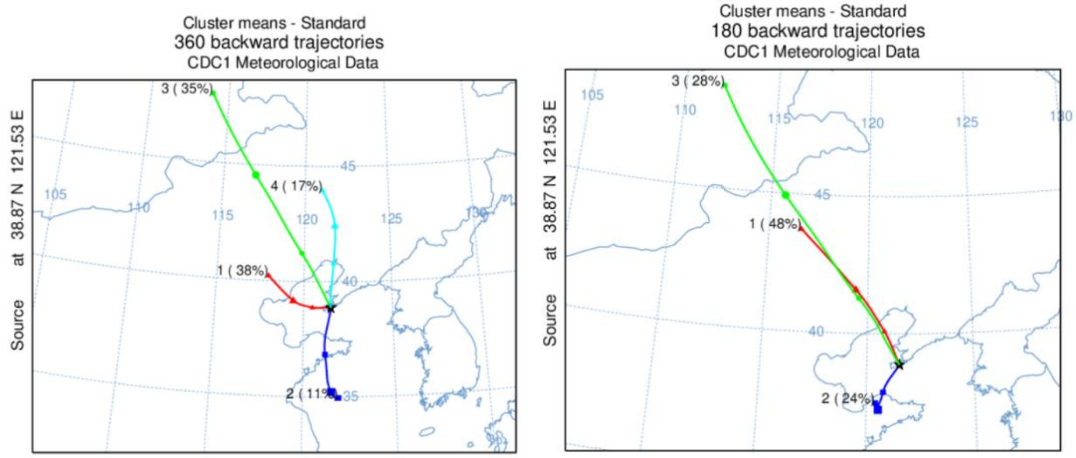

DL 2016winter

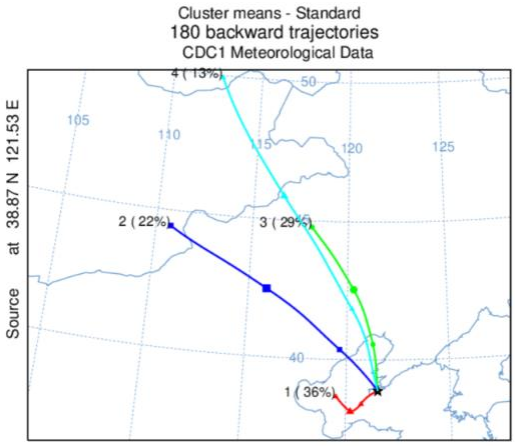

DL 2017winter

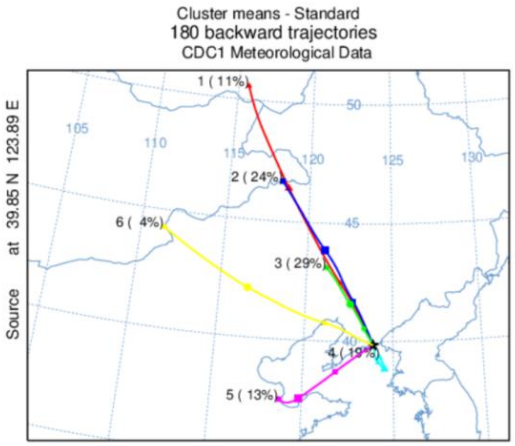

DL 2018winter

DG 2014winter

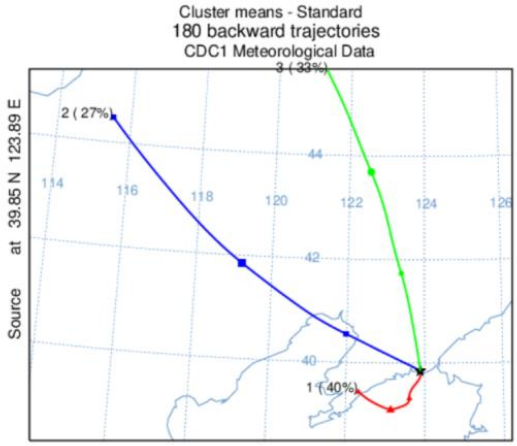

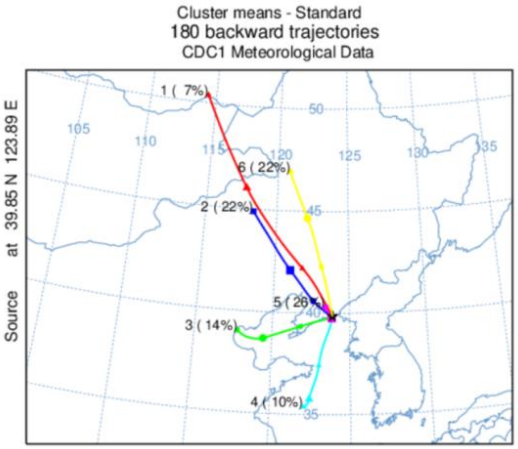

DG 2015winter

DG 2016winter

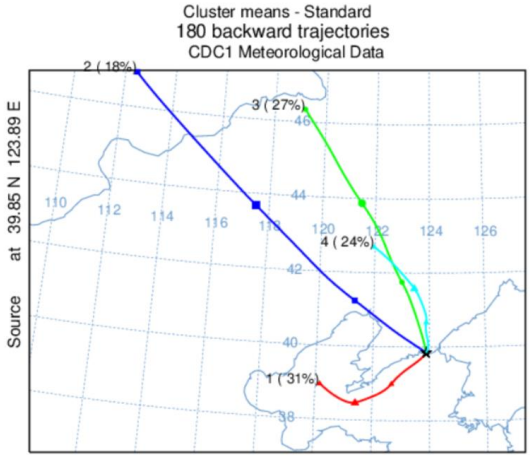

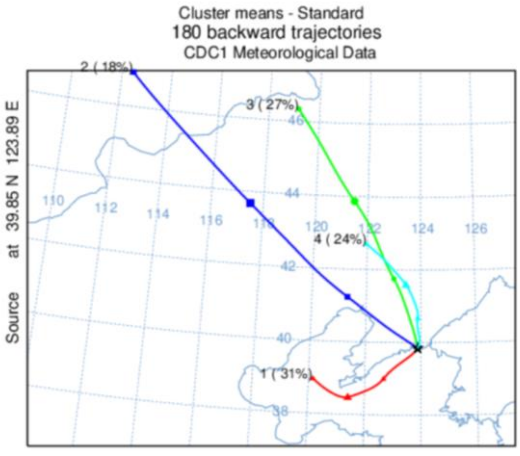

DG 2017winter

DG 2018winter

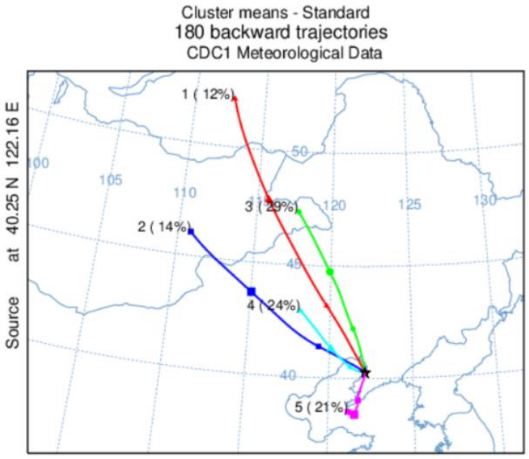

GZ 2014winter

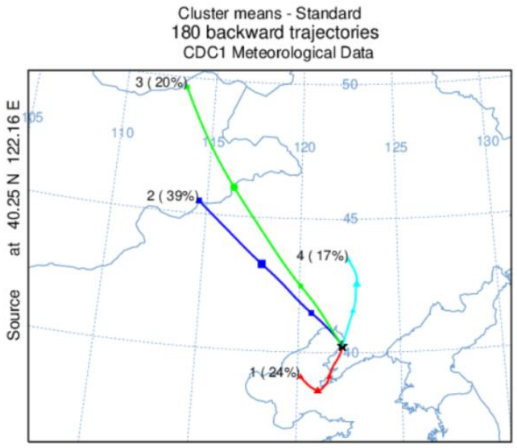

GZ 2015winter

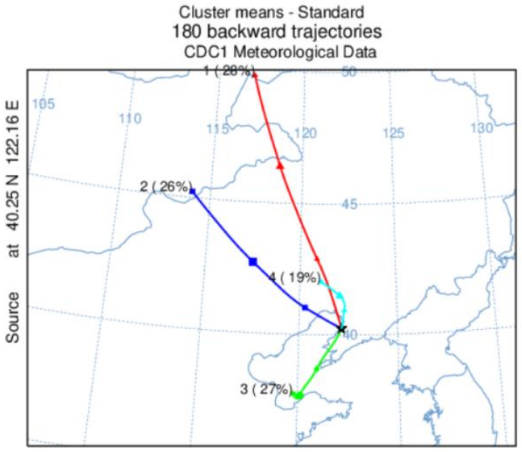

GZ 2016winter

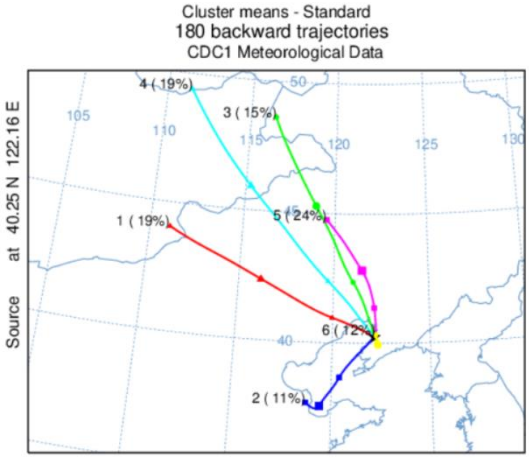

GZ 2017winter

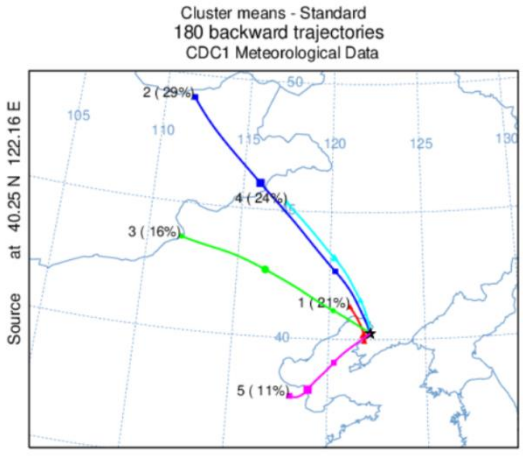

GZ 2018winter

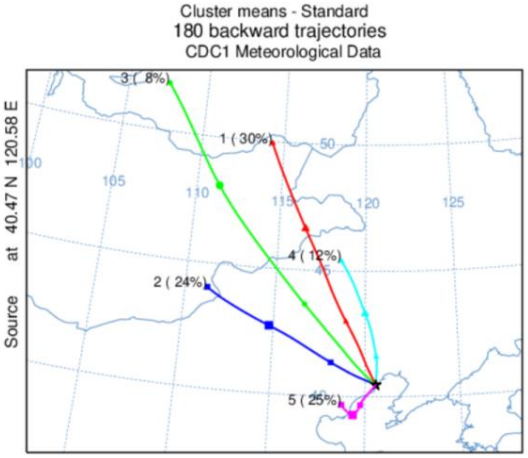

XC 2014winter

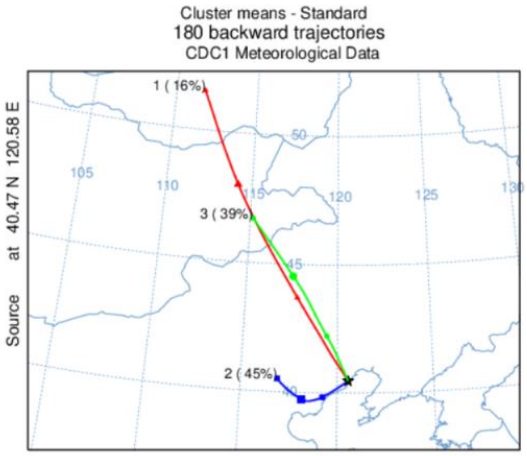

XC 2015winter

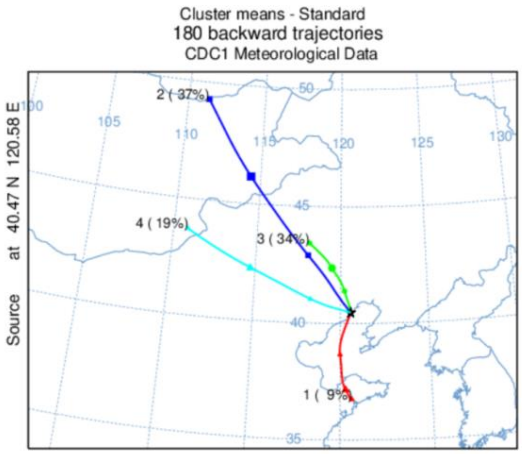

XC 2016winter

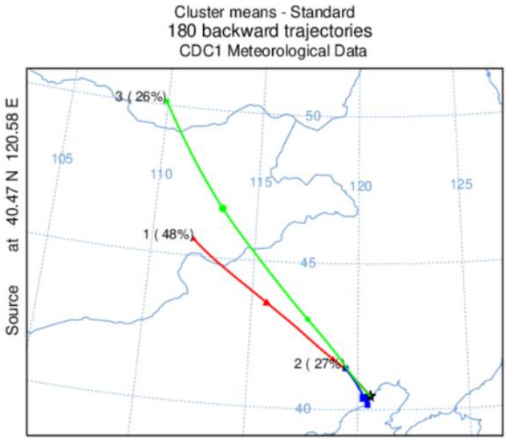

XC 2017winter

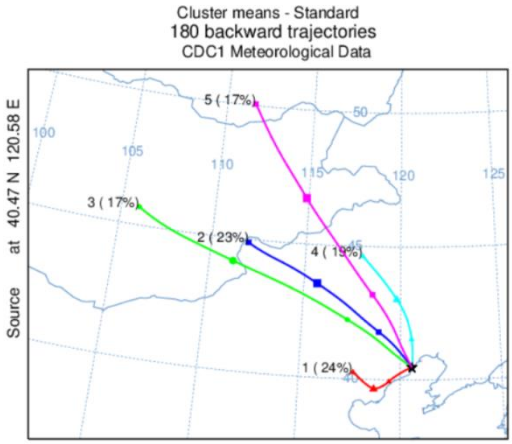

XC 2018winter

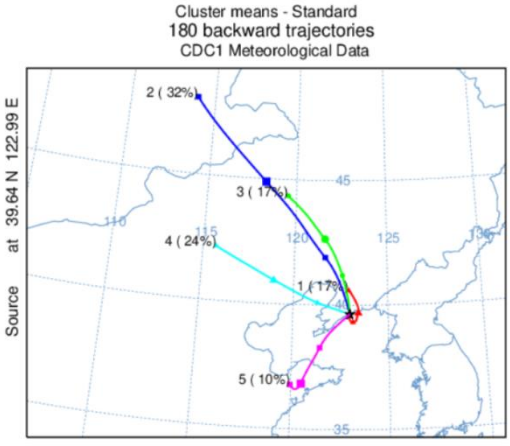

ZH 2014winter

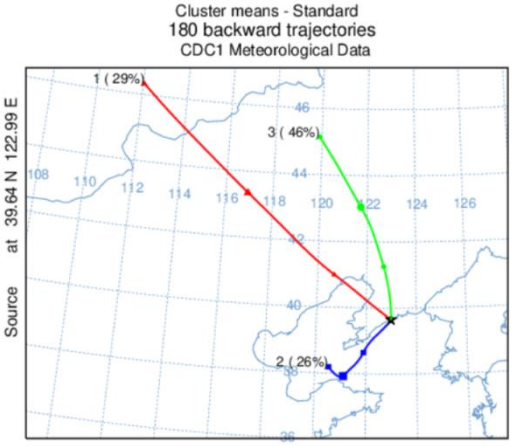

ZH 2015winter

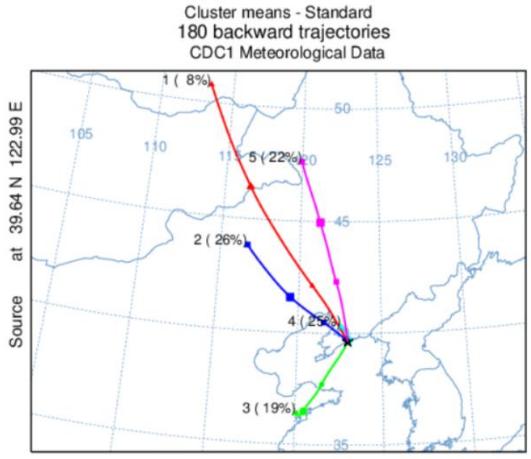

ZH 2016winter

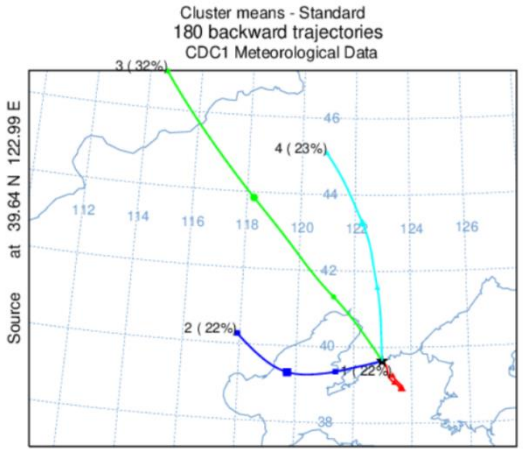

ZH 2017winter

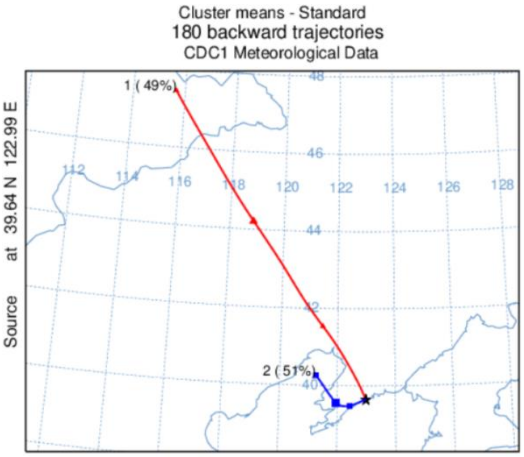

ZH 2018winter

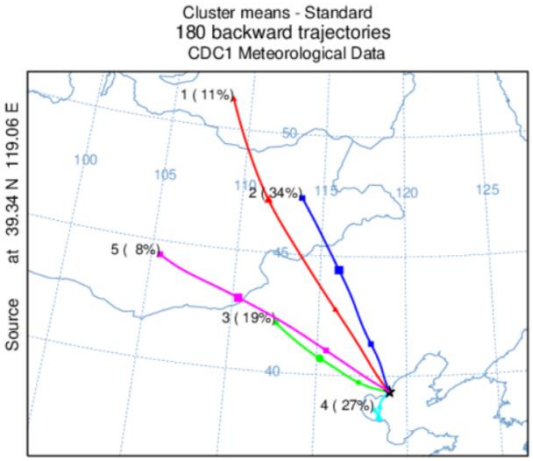

LT 2014winter

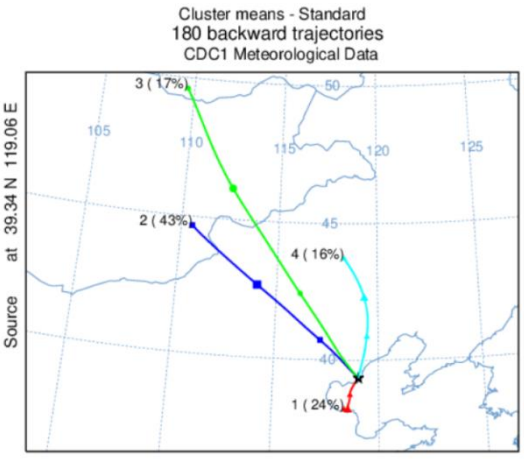

LT 2015winter

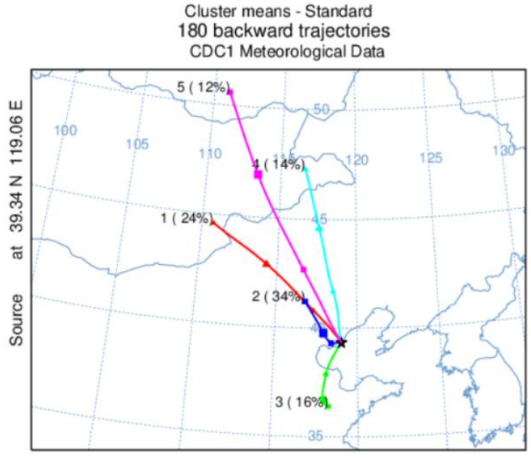

LT 2016winter

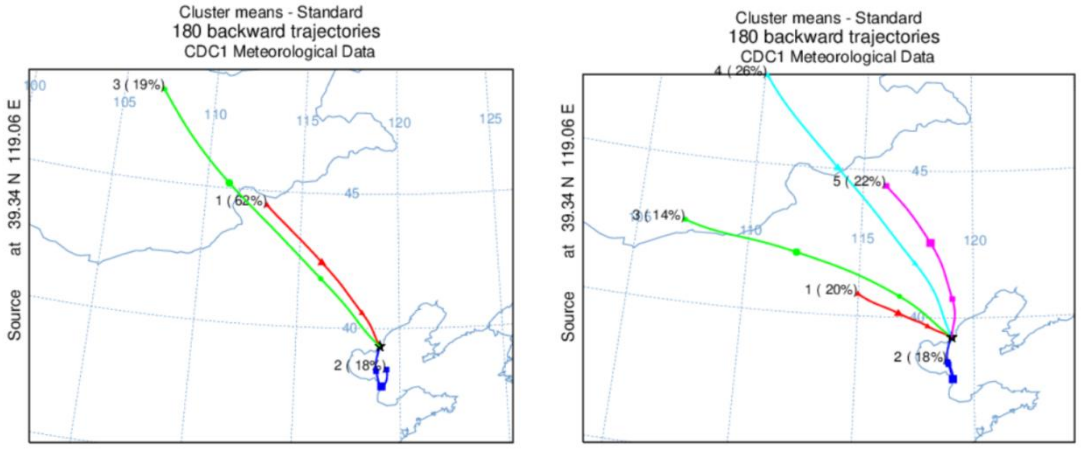

LT 2017winter LT 2018winter

Figure S4. The backward trajectory by Hysplit model of the northern Bohai Sea sites in winter.

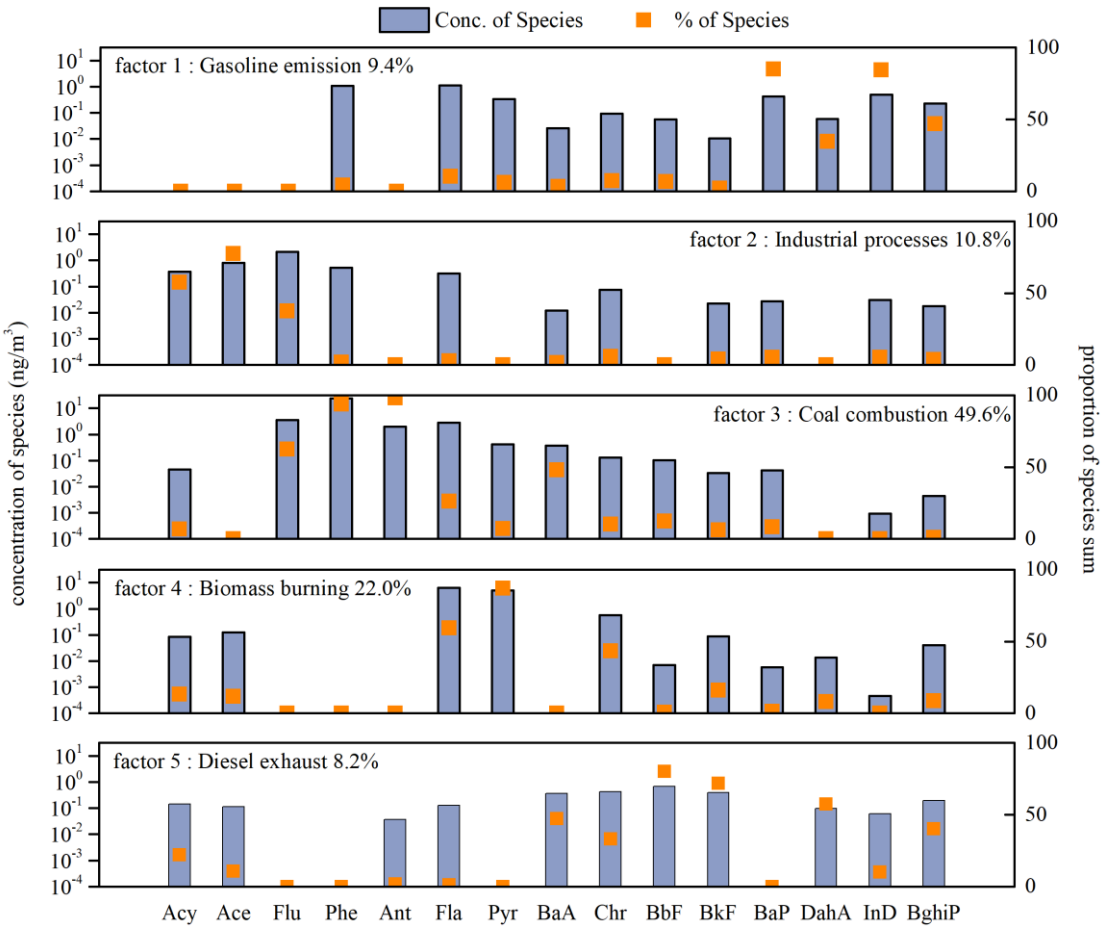

Figure S5. Factor profiles of PAHs by the PMF model.

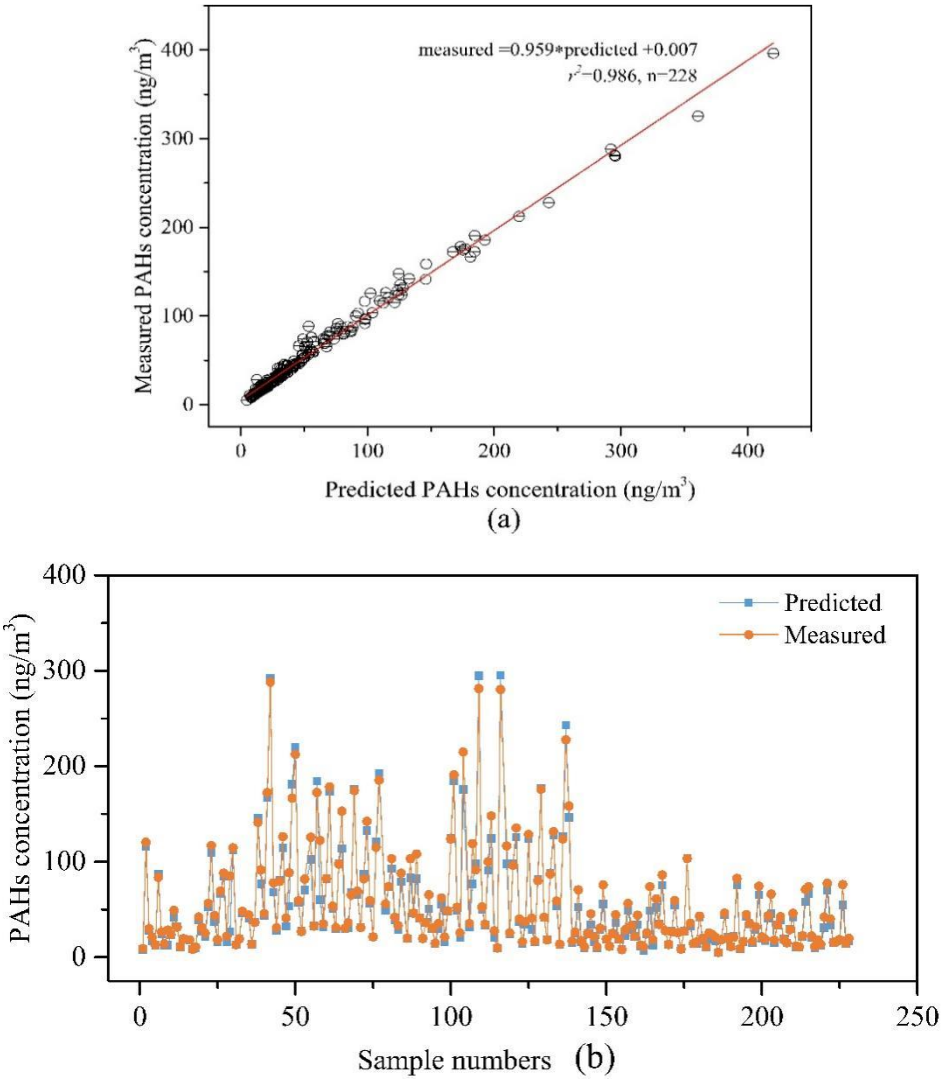

Figure S6. The relationship between predicted and measured concentrations of 228 samples analyzed by PMF (a) and (b).

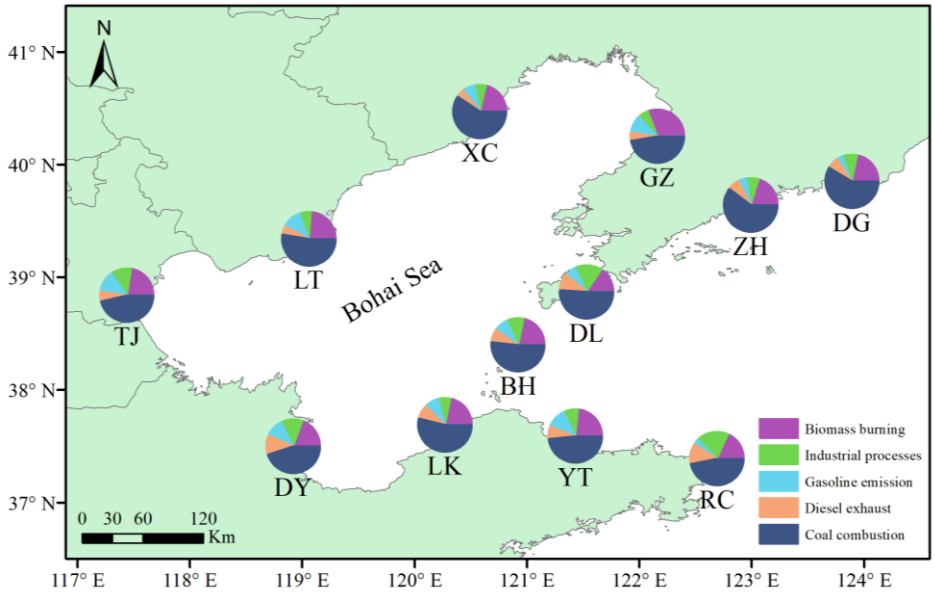

Figure S7. The average contributions of the five sources of PAHs at 12 sites around the BS.

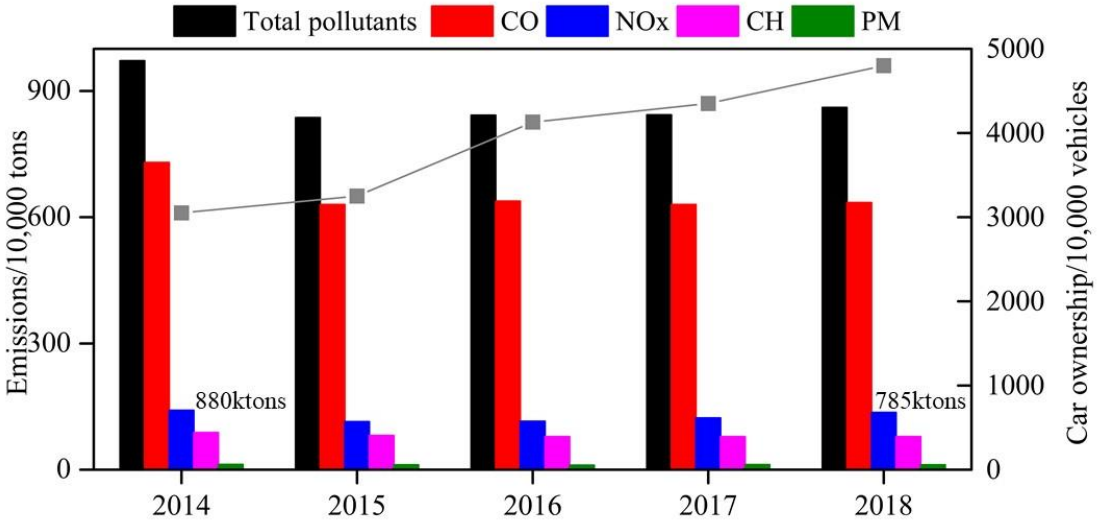

Figure S8. The pollutants emissions of motor vehicle around the BS within five years.

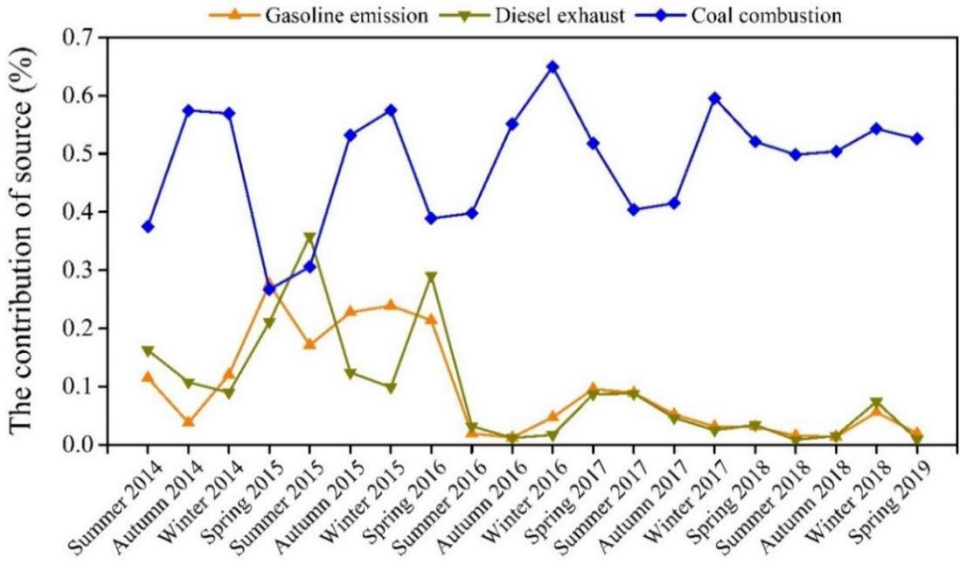

Figure S9. Seasonal contribution of coal combustion and vehicle emission for PAHs around the BS.

References

Chen, P.F., Li, C.L., Kang, S.C., Yan, F.P., Zhang, Q.G., Ji, Z.M., Tripathee, L., Rupakheti, D., Rupakheti, M., Qu, B., and Sillanpaa, M.: Source apportionment of particle-bound polycyclic aromatic hydrocarbons in Lumbini, Nepal by using the positive matrix factorization receptor model, Atmos. Res., 182, 46–53, https://doi.org/10.1016/j.atmosres.2016.07.011, 2016.

Chueinta, W., Hopke, P.K., and Paatero, P.: Investigation of sources of atmospheric aerosol at urban and suburban residential areas in Thailand by positive matrix factorization, Atmos. Environ., 34, 3319–3329, https://doi.org/10.1016/s1352-2310(99)00433-1, 2000.

Gong, P., Wang, X.P., Sheng, J.J., Wang, H.L., Yuan, X.H., He, Y.Q., Qian, Y., and Yao, T.D.: Seasonal variations and sources of atmospheric polycyclic aromatic hydrocarbons and organochlorine compounds in a high-altitude city: Evidence from four-year observations, Environ. Pollut., 233, 1188–1197, https://doi.org/10.1016/j.envpol.2017.10.064, 2018.

Guarieiro, A.L.N., Santos, J.V.D., Eiguren-Fernandez, A., Torres, E.A., da Rocha, G.O., and de Andrade, J.B.: Redox activity and PAH content in size-classified nanoparticles emitted by a diesel engine fuelled with biodiesel and diesel blends, Fuel., 116, 490–497, https://doi.org/10.1016/j.fuel.2013.08.029, 2014.

He, L.Y., Hu, M., Zhang, Y.H., Huang, X.F., and Yao, T.T.: Fine particle emissions from on-road vehicles in the Zhujiang Tunnel, China, Environ. Sci. Technol., 42, 4461–4466, https://doi.org/10.1021/es7022658, 2008.

Huang, W., Huang, B., Bi, X.H., Lin, Q.H., Liu, M., Ren, Z.F., Zhang, G.H., Wang, X.M., Sheng, G.Y., and Fu, J.M.: Emission of PAHs, NPAHs and OPAHs from residential honeycomb coal briquette combustion, Energ. Fuel., 28, 636–642. https://doi.org/10.1021/ef401901d, 2014.

Jenkins, B.M., Jones, A.D., Turn, S.Q., and Williams, R.B.: Emission factors for polycyclic aromatic hydrocarbons from biomass burning, Environ. Sci. Technol., 30, 2462–2469, https://doi.org/10.1021/es950699m, 1996.

Kim, E., Hopke, P.K., Larson, T.V., and Covert, D.S.: Analysis of ambient particle size distributions using unmix and positive matrix factorization, Environ. Sci. Technol., 38, 202–209, https://doi.org/10.1021/es030310s, 2004.

Kong, S.F., Ji, Y.Q., Li, Z.Y., Lu, B., and Bai, Z.P.: Emission and profile characteristic of polycyclic aromatic hydrocarbons in $PM_{2.5}$ and PM_{10} from stationary sources based on dilution sampling, Atmos. Environ., 77, 155–165, https://doi.org/10.1016/j.atmosenv.2013.04.073, 2013.

Ma, W.L., Li, Y.F., Qi, H., Sun, D.Z., Liu, L.Y., and Wang, D.G.: Seasonal variations of sources of

polycyclic aromatic hydrocarbons (PAHs) to a northeastern urban city, China, Chemosphere., 79, 441–447, https://doi.org/10.1016/j.chemosphere.2010.01.048, 2010.

Nisbet, I.C.T., and Lagoy, P.K.: Toxic Equivalency Factors (TEFS) for Polycyclic Aromatic-Hydrocarbons (PAHS), Regul. Toxicol. Pharm., 16, 290–300, https://doi.org/10.1016/0273-2300(92)90009-x, 1992.

Ray, D., Chatterjee, A., Majumdar, D., Ghosh, S.K., and Raha, S.: Polycyclic aromatic hydrocarbons over a tropical urban and a high latitude Himalayan Station in India: Temporal variation and source apportionment, Atmos. Res., 197, 331–341, https://doi.org/10.1016/j.atmosres.2017.07.010, 2017.

Riddle, S.G., Jakober, C.A., Robert, M.A., Cahill, T.M., Charles, M.J., and Kleeman, M.J.: Large PAHs detected in fine particulate matter emitted from light-duty gasoline vehicles, Atmos. Environ., 41, 8658–8668, https://doi.org/10.1016/j.atmosenv.2007.07.023, 2007.

Shen, H., Huang, Y., Wang, R., Zhu, D., Li, W., Shen, G., Wang, B., Zhang, Y., Chen, Y., Lu, Y., Chen, H., Li, T., Sun, K., Li, B., Liu, W., Liu, J., and Tao, S.: Global atmospheric emissions of polycyclic aromatic hydrocarbons from 1960 to 2008 and future predictions, Environ. Sci. Technol., 47, 6415–6424, https://doi.org/10.1021/es400857z, 2013.

Tobiszewski, M., and Namiesnik, J.: PAH diagnostic ratios for the identification of pollution emission sources, Environ. Pollut., 162, 110–119, https://doi.org/10.1016/j.envpol.2011.10.025, 2012.

Wang, D.G., Tian, F.L., Yang, M., Liu, C.L., and Li, Y.F.: Application of positive matrix factorization to identify potential sources of PAHs in soil of Dalian, China, Environ. Pollut., 157, 1559–1564, https://doi.org/10.1016/j.envpol.2009.01.003, 2009.

Westerholm, R., Christensen, A., Tornqvist, M., Ehrenberg, L., Rannug, U., Sjogren, M., Rafter, J., Soontjens, C., Almen, J., and Gragg, K.: Comparison of exhaust emissions from Swedish environmental classified diesel fuel (MK1) and European Program on Emissions, Fuels and Engine Technologies (EPEFE) reference fuel: A chemical and biological characterization. with viewpoints on cancer risk, Environ. Sci. Technol., 35, 1748–1754, https://doi.org/10.1021/es000113i, 2001.

Wu, D., Wang, Z.S., Chen, J.H., Kong, S.F., Fu, X., Deng, H.B., Shao, G.F., and Wu, G.: Polycyclic aromatic hydrocarbons (PAHs) in atmospheric $PM_{2.5}$ and PM_{10} at a coal-based industrial city: Implication for PAH control at industrial agglomeration regions, China, Atmos. Res., 149, 217–229, https://doi.org/10.1016/j.atmosres.2014.06.012, 2014.

Yunker, M.B., Macdonald, R.W., Vingarzan, R., Mitchell, R.H., Goyette, D., and Sylvestre, S.: PAHs in the Fraser River basin: a critical appraisal of PAH ratios as indicators of PAH source and composition, Org. Geochem., 33, 489–515, https://doi.org/10.1016/s0146-6380(02)00002-5, 2002.

Zhu, L.Z., Wang, J., Du, Y., and Xu, Q.Q.: Research on PAHs fingerprints of vehicle discharges, Environmental Science (China), 3, 26–29, https://doi.org/10.13227/j.hjkx.2003.03.005, 2003.

Zhu, Y., Yang, L., Yuan, Q., Yan, C., Dong, C., Meng, C., Sui, X., Yao, L., Yang, F., Lu, Y., and Wang, W.: Airborne particulate polycyclic aromatic hydrocarbon (PAH) pollution in a background site in the North China Plain: concentration, size distribution, toxicity and sources, Sci. Total. Environ., 466-467, 357–368, https://doi.org/10.1016/j.scitotenv.2013.07.030, 2014.